

# Favor changing effects on single charged Higgs boson production associated with a bottom-charm pair at CERN Large Hadron Collider

Sun Hao, Ma Wen-Gan, Zhang Ren-You, Guo Lei, Han Liang and Jiang Yi

Department of Modern Physics, University of Science and Technology  
of China (USTC), Hefei, Anhui 230026, P.R. China

## Abstract

We study flavor changing effects on the  $pp \rightarrow b\bar{b}H + X$  process at the Large Hadron Collider (LHC), which are inspired by the left-handed up-type squark mixings in the Minimal Supersymmetric Standard Model (MSSM). We find that the SUSY QCD radiative corrections to  $b\bar{b}H$  coupling can significantly enhance the cross sections at the tree-level by a factor about 1.5–5 with our choice of parameters. We conclude that the squark mixing mechanism in the MSSM makes the  $pp \rightarrow b\bar{b}H + X$  process a new channel for discovering a charged Higgs boson and investigating flavor changing effects.

PA SC : 12.60.Jv, 14.80.Cp, 14.65.Fy

---

Supported by National Natural Science Foundation of China.

## I Introduction

As we know there are stringent experimental constraints against the existence of tree-level flavor changing scalar interactions (FC SI's) for light quarks. It leads to the suppression of the flavor changing neutral current (FCNC) couplings at the lowest order. This is also an important feature of the standard model (SM) [1]. Even the one-loop flavor changing effect in the SM is still small, due to the suppression of the Glashow-Iliopoulos-Maiani (GIM) mechanism [2]. In extension models beyond the SM when new non-standard particles exist in the loops, significant contributions to flavor changing transitions may appear. Among various new physics models, the minimal supersymmetric extension (MSSM) [3] is widely considered as the one of the most appealing extensions of the SM. The MSSM not only can explain the existing experimental data as the SM does, but also can be used to solve various theoretical problems in the SM, such as the huge hierarchy problem between the electroweak symmetry-breaking and the grand unification scales. In the MSSM there exist two Higgs doublets to break the electroweak symmetry. After symmetry breaking, there are five physical Higgs bosons: two CP-even Higgs bosons ( $h^0, H^0$ ), one CP-odd boson ( $A^0$ ) and two charged Higgs bosons ( $H^\pm$ ) [4]. Significant difference exists between the couplings involving Higgs boson in the MSSM and those in the SM. In SUSY models, an important feature is that the fermion-Higgs couplings are no longer strictly proportional only to the corresponding mass as they are in the SM. For example, the b-quark coupling with neutral Higgs boson  $A^0$  in the MSSM becomes enhanced for large  $\tan\beta = v_2/v_1$ , the ratio of the two vacuum expectation

values[4]. Thus, di erent features can be presented due to the existence of the ve Higgs bosons in the M SSM which might lead di erent coupling strengths, decay widths and production cross sections compared with in the SM .

The understanding of avor sector is a major challenge for various extension models of the SM . In the M SSM , them inimal avorviolation is realized by the CKM - matrix[5]. While in the general M SSM with avorviolation, a possible avormixings between the three sferm ion generations are allowed and lead to avor changing e ects. The avor changing e ects originating from such sferm ion-mixing scenario normally cannot be generated at the tree-level, but could show up at the one-loop level and induce signi cant contributions to be observed in speci c regions of the M SSM parameters.

Searching for scalar Higgs bosons is one of the major objectives of present and future high energy experiments. In most extensions of the SM , the mass of a charged Higgs boson ( $m_H$  ) is predicted to be around the weak scale. However, the Higgs bosons haven't been directly explored experimentally until now . At hadron colliders, such as the Fermilab Tevatron and the CERN Large Hadron Collider(LHC ), a light charged Higgs boson can be produced from the decay of top quark via  $t \rightarrow H^+ b$ , if  $m_H < m_t - m_b$ [6]. Otherwise, if the charged Higgs boson is heavier than top quark, there are three major channels to search for charged Higgs boson: (1) charged Higgs boson pair production [7, 8, 9]; (2) associated production of a charged Higgs boson with a W boson [10]; (3) associated production of a charged Higgs boson with a top quark  $g b \rightarrow t H$  [11]; (4) single charged Higgs production  $cs; db \rightarrow H$  [12]. The decay of the charged Higgs boson has two major channels:  $H \rightarrow tb$ [13], and

H ! [4]. At the LHC, the most promising channel to search for the charged Higgs boson in some specific parameter space, is  $pp \rightarrow b\bar{b}H + X$ , whose QCD corrections have been studied in Ref.[5, 16, 17]. The  $pp \rightarrow b\bar{b}H + X$  process is another important alternative channel especially considering the contributions from squark-guino loops with flavor mixing structure. J.L. Diaz-Cruz, et al., analyzed SUSY radiative corrections to the  $b\bar{b}H$  and  $t\bar{t}H^0$  couplings including squark mixing effects, and showed that these couplings can reveal exciting new discovery channels for the Higgs boson signals at the Tevatron and the LHC [12]. H.J. He, et al., studied the single charged Higgs production process at linear colliders, such as  $e^-e^+ \rightarrow b\bar{b}H^+$ ,  $H^+$  and  $\tau^-\tau^+ \rightarrow b\bar{b}H^+$ ,  $H^+$  [18]. The flavor changing effect on the neutral Higgs boson production associated with a bottom-strange quark pair in the MSSM at the linear collider was studied in Ref.[19].

As we know, among the three generations of fermions, the top-quark is the heaviest one with its mass as high as the electroweak scale. The large top-quark mass will enhance flavor changing Yukawa coupling  $b\bar{b}H$  at the loop level and make the single charged Higgs production process  $pp \rightarrow b\bar{b}H + X$  to be an important channel for probing flavor violation and searching for charged Higgs boson at hadron colliders. Furthermore, when the neutral scalar ( $H^0$ ) and the charged scalar ( $H^\pm$ ) form a  $SU(2)$  doublet, the weak isospin symmetry connects the flavor-changing neutral coupling (FCNC)  $tc^0$  to the flavor-mixing charged coupling (FMCC)  $bc^\pm$  through the (s)quark-mixing matrix. Therefore, if we can directly measure the coupling of FMCC at future high energy colliders, it would provide the detailed information on the FCNC and may give more precise constraints on the FCNC than that inferred

from kaon and bottom physics obtained from low energy experiments.

Although the electroweak corrections can contribute to the flavor changing effect on the process  $pp \rightarrow b\bar{b}H \rightarrow X$ , but the SUSY QCD corrections via squark-gluino loops are dominant over the previous ones, at least one order larger in magnitude. In this work, we calculate the single charged Higgs boson production process associated with a bottom-charm pair  $pp \rightarrow b\bar{b}H \rightarrow X$  in the MSSM with left-handed up-type squark mixings at QCD one-loop level at the CERN LHC. We shall show the importance of squark-mixings in the enhancement of production rate for  $pp \rightarrow b\bar{b}H \rightarrow X$  process. We analyze the SUSY QCD radiative contributions to the process  $pp \rightarrow b\bar{b}H \rightarrow X$  by adopting the relevant MSSM parameters at the Snowmass point SPS 4 with large  $\tan\beta$ . The paper is organized as below: In section 2 we present a brief outline on the up-type squark mass matrix considering the left-handed up-type squark mixings, and diagonalize it to obtain the mass eigenstates matrix of squarks. In section 3, we give the calculations of the cross sections of  $pp \rightarrow b\bar{b}H \rightarrow X$  up to the order  $O(gg_s^4)$  in the MSSM. The numerical results and discussions are presented in section 4. Finally, a short summary is given.

## II Left-Handed Up-Type Squark Mixing

In the supersymmetric models, the SM flavor mixings between quarks of three generations can be extended to include the superpartners of quarks and leptons by introducing the supersymmetry soft-breaking mechanism. These models leave further puzzles to the flavor physics, since the soft-breaking Lagrangian of the supersymmetric, which gives a mass spectrum of the supersymmetric particles, involves numerous

unconstrained free parameters. In order to fit with low-energy FCNC data, we have to make specific assumptions to these free parameters.

In the study of the  $b\bar{b}H$  production at hadron colliders, only the flavor mixing in squark sector is concerned. For the down-type squark mixings, there are possible strong constraints on the mixing parameters from the low-energy experimental data. For example, the mechanism with down-type squark mixings in large  $\tan\beta$  could enhance the FCNC  $B^-$  decays by several orders[20] and seems to be ruled out by  $B$ -factory experiments. But the up-type squark mixing between  $\tilde{t}$  and  $\tilde{c}$  is subject to no strong low-energy constraint[21]. Such  $\tilde{t}\tilde{c}$  squark mixing is well-motivated in low-energy supergravity models (SUGRA)[22]. Ref.[23] shows that at low energy the  $\tilde{t}\tilde{c}$  mixing may be significant due to very heavy top quark, and the mixing between  $\tilde{t}_L$  and  $\tilde{c}_L$  is most likely to be large, which is proportional to a sum of some soft masses. For theoretical simplicity in this work, we focus on the MSSM with the squark-mixing assumption that only the left-handed up-type squarks in three generations can mix with each other[24]. In the super Cabibbo-Kobayashi-Maskawa (CKM) basis  $U^0 = (\tilde{u}_L; \tilde{d}_R; \tilde{c}_L; \tilde{s}_R; \tilde{t}_L; \tilde{b}_R)$ , the  $6 \times 6$  squark mass matrix  $M_U^2$  of up-type squark sector takes the form as[25]

$$M_U^2 = \begin{pmatrix} 0 & M_{L,u}^2 & a_u m_u & 12 M_{L,u} M_{L,c} & 0 & 31 M_{L,u} M_{L,\tau} & 0 & 1 \\ B & a_u m_u & M_{R,u}^2 & 0 & 0 & 0 & 0 & B \\ B & 12 M_{L,c} M_{L,u} & 0 & M_{L,c}^2 & a_c m_c & 23 M_{L,c} M_{L,\tau} & 0 & C \\ B & 0 & 0 & a_c m_c & M_{R,c}^2 & 0 & 0 & C \\ C & 31 M_{L,\tau} M_{L,u} & 0 & 23 M_{L,\tau} M_{L,c} & 0 & M_{L,\tau}^2 & a_t m_t & A \\ C & 0 & 0 & 0 & 0 & a_t m_t & M_{R,\tau}^2 & A \end{pmatrix} \quad (2.1)$$

where

$$\begin{aligned}
 M_{L,q}^2 &= M_{\tilde{q},q}^2 + m_z^2 \cos^2 \left( \frac{1}{2} \tan \theta_w \sin^2 \theta_w \right) + m_q^2; \\
 M_{R,q}^2 &= M_{\tilde{q},q}^2 + Q_q m_z^2 \cos^2 \theta_w \sin^2 \theta_w + m_q^2; \\
 a_q &= A_q \cot \theta_w; \quad (q = u, c, t); \quad (2.2)
 \end{aligned}$$

with  $m_z$  being the mass of  $Z^0$ , and  $m_q, Q_q$  the up-quark mass and charge.  $M_{\tilde{q},q}$  and  $M_{\tilde{q},q}$  are mass parameters of supersymmetry soft breaking.  $A_q$  ( $q = u, c, t$ ) are the trilinear scalar coupling parameters of Higgs boson with two scalar quarks.  $\tan \theta_w$  is the mass parameter of the Higgs boson sector and  $\tan \theta_w$  is the ratio of the vacuum expectation values in this sector.  $\sin \theta_w$  contains the electroweak mixing angle  $\theta_w$ .  $\alpha_{12}, \alpha_{23}$  and  $\alpha_{31}$  are the avormixing strengths of the  $\tilde{u}_L - \tilde{c}_L$ ,  $\tilde{c}_L - \tilde{t}_L$  and  $\tilde{t}_L - \tilde{u}_L$  sectors, respectively. Since we don't consider the CP violation, all these squark-mixing parameters have real and positive values varying in the range of  $[0; 1]$ .

To obtain the mass eigenstates of the up-type squarks, we should introduce an unitary matrix  $R^{(U)}$  defined as

$$U^0 = R^{(U)} U; \quad (2.3)$$

where

$$U^0 = \begin{pmatrix} 0 & 1 \\ \tilde{u}_L & \tilde{c}_L \\ \tilde{c}_R & \tilde{t}_L \\ \tilde{t}_R & A \end{pmatrix}; \quad U = \begin{pmatrix} 0 & 1 & 0 & 1 \\ \tilde{u}_1 & \tilde{c}_1 & \tilde{u}_1 & \tilde{c}_1 \\ \tilde{u}_2 & \tilde{c}_2 & \tilde{u}_2 & \tilde{c}_2 \\ \tilde{u}_3 & \tilde{c}_3 & \tilde{u}_3 & \tilde{c}_3 \\ \tilde{u}_4 & \tilde{c}_4 & \tilde{u}_4 & \tilde{c}_4 \\ \tilde{u}_5 & \tilde{c}_5 & \tilde{u}_5 & \tilde{c}_5 \\ \tilde{u}_6 & \tilde{c}_6 & \tilde{u}_6 & \tilde{c}_6 \end{pmatrix} = \begin{pmatrix} 0 & 1 \\ \tilde{u}_1 & \tilde{c}_1 \\ \tilde{u}_2 & \tilde{c}_2 \\ \tilde{u}_3 & \tilde{c}_3 \\ \tilde{u}_4 & \tilde{c}_4 \\ \tilde{u}_5 & \tilde{c}_5 \\ \tilde{u}_6 & \tilde{c}_6 \end{pmatrix}; \quad (2.4)$$

The up-squark mass matrix  $M_{\tilde{q}}^2$  is diagonalized by the  $6 \times 6$  matrix  $R^{(U)}$  via

$$R^{(U)} M_{\tilde{q}}^2 R^{(U)} = \text{diag} m_{\tilde{u}_1}^2, \dots, m_{\tilde{u}_6}^2; \quad (2.5)$$

where  $m_{\tilde{q}_j}^2$  ( $j = 1, \dots, 6$ ) are the masses of mass eigenstates of the six up-type squarks which depend on  $m_{12}$ ,  $m_{23}$  and  $m_{31}$ .

### III Calculation of the process $pp \rightarrow b\bar{c}H \rightarrow X$

The exclusive process of single charged Higgs boson production associated with a bottom-charm quark pair,  $pp \rightarrow b\bar{c}H \rightarrow X$ , involves the contributions from the subprocesses of  $q\bar{q}$  ( $q = u, d, c, s$ ) annihilation and gluon-gluon fusion. Since the processes  $q\bar{q} \rightarrow gg \rightarrow b\bar{c}H$  have the same total and differential cross sections as their corresponding charge-conjugate subprocesses  $q\bar{q} \rightarrow gg \rightarrow b\bar{c}H$  in the CP-conserving MSSM, we present here only the calculations of the process  $pp \rightarrow b\bar{c}H \rightarrow X$ . For each subprocesses of  $q\bar{q} \rightarrow b\bar{c}H$  and  $gg \rightarrow b\bar{c}H$ , we depict one tree-level ( $O(gg_s^2)$ ) Feynman diagram as a demonstration in Fig. 1(1) and Fig. 1(2), respectively.

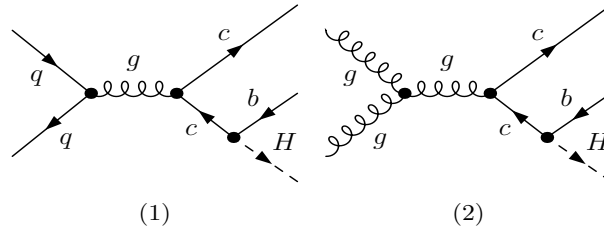


Figure 1: (1) One of the tree-level ( $O(gg_s^2)$ ) Feynman diagrams for  $q\bar{q} \rightarrow b\bar{c}H$  subprocess. (2) One of the tree-level ( $O(gg_s^2)$ ) Feynman diagrams for  $gg \rightarrow b\bar{c}H$  subprocess.

The tree-level total cross section of  $pp \rightarrow b\bar{c}H \rightarrow X$  can be obtained by doing following integration:

$$\sum_{ij=uu,dd} \text{tree}(pp(A B) \rightarrow b\bar{c}H \rightarrow X) = \frac{1}{1 + \frac{1}{\int dx_A dx_B [G_{i=A}(x_A; f) G_{j=B}(x_B; f) \hat{\chi}_{\text{tree}}^{ij}(x_A; x_B; f) + (A \leftrightarrow B)]]} \quad (3.1)$$

where  $x_A$  and  $x_B$  are defined as

$$x_A = \frac{p_1}{P_A}; x_B = \frac{p_2}{P_B}; \quad (3.2)$$

where A and B represent the incoming colliding protons.  $p_1, p_2, P_A$  and  $P_B$  are the momenta of partons and protons.  $\hat{\sigma}_{\text{tree}}^{ij}$  ( $ij = uu; dd; cc; ss; gg$ ) is the total LO cross section at parton-level for incoming  $i$  and  $j$  partons.  $G_{i=A(B)}$  is the leading-order parton distribution function (PDF) for parton  $i$  in hadron A (B). We adopt CTEQ 6L1 PDF in the calculation of the tree-level cross section [26].

In the calculation of the SUSY QCD NLO contributions in the framework of the MSSM with left-handed up-type squark mixings, we adopt the 'tHooft-Feynman gauge, and use dimensional regularization (DR) method in  $D = 4 - 2$  dimensions to isolate the ultraviolet (UV), soft and collinear infrared (IR) singularities. The modified minimal subtraction ( $\overline{MS}$ ) scheme is employed to renormalize and eliminate UV divergencies. The SUSY QCD NLO contributions can be divided into two parts: the virtual contributions from one-loop diagrams, and the real gluon/light-quark emission contributions.

The unrenormalized virtual contribution to the subprocess  $q\bar{q} \rightarrow gg + b\bar{b}H$  in the MSSM consists of self-energy, vertex, box, and pentagon diagrams. These one-loop diagrams for subprocess  $q\bar{q} \rightarrow gg + b\bar{b}H$  can be divided into two parts: One is the SM-like part which comprises the diagrams including gluon/quark loops. Another is called SUSY part involving virtual gluino/squark exchange loops. In the later part, contributions from the one-loop diagrams with left-handed up-type squark mixings between different generations are considered. For demonstration, we plot

the QCD one-loop pentagon diagrams for the  $gg \rightarrow b\bar{b}H^+$  subprocess in Fig.2. The figures in Fig.2(1)–(12) belong to the SM-like part, while Fig.2(13)–(24) to the SUSY part. The amplitude for the virtual SM-like contribution part contains both ultraviolet (UV) and soft/collinear infrared (IR) singularities, while the amplitude corresponding to SUSY loop part contains only UV singularities. In order to remove the UV divergences, we renormalize the relevant fields, the masses of charm- and bottom-quark in propagators and the  $b\bar{b}H$  Yukawa coupling by adopting on-shell(OS) scheme. The renormalization constants of the CKM matrix elements  $V_{ij}$  ( $i, j = 1, 2, 3$ ) can be obtained by keeping the unitarity of the renormalized CKM matrix, and expressed as[27]

$$V_{ij} = \frac{1}{4} \frac{h}{Z_{ik}^{u,L} Z_{ik}^{u,L,Y} V_{kj} V_{ik} Z_{kj}^{d,L} Z_{kj}^{d,L,Y}} : \quad (3.3)$$

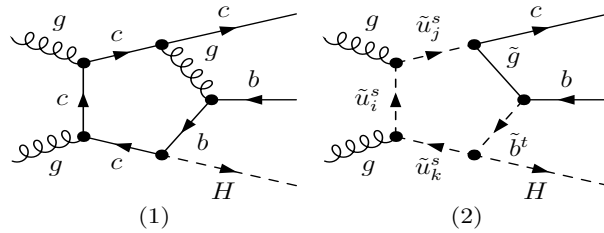


Figure 2: The representative QCD pentagon Feynman diagrams for  $gg \rightarrow b\bar{b}H$  subprocess. (1) is the SM-like diagram, and (2) is the SUSY QCD one-loop diagram. The lower-index  $i$  in  $\tilde{u}_i^s$  implies the  $i$ -th generation ( $i = 1, 2, 3$ ) and the upper-index  $s = 1, 2$ .

We use the  $\overline{MS}$  mass of the bottom quark ( $\tilde{m}_b(r)$ ) in  $b\bar{b}H$  Yukawa coupling, to absorb the large logarithms contributions which arise from the renormalization of bottom quark mass[30], but keep the bottom quark pole mass everywhere else. The bottom quark mass in propagator is renormalized by adopting the on-shell(OS)

scheme. The expressions of the  $\overline{MS}$  mass of the bottom quark  $\overline{m}_b(r)$  corresponding 1-loop and 2-loop renormalization groups are given by

$$\overline{m}_b(r)_{1\text{ loop}} = m_b \frac{s(r)}{s(m_b)}^{c_0=b_0}; \quad (3.4)$$

$$\overline{m}_b(r)_{2\text{ loop}} = m_b \frac{s(r)}{s(m_b)}^{c_0=b_0} \left( 1 + \frac{c_0}{b_0} (c_1 - b_1) \frac{s(r)}{s(m_b)} \right) \left( 1 - \frac{4}{3} \frac{s(m_b)}{s(r)} \right); \quad (3.5)$$

where

$$\begin{aligned} b_0 &= \frac{1}{4} - \frac{11}{3} N_c - \frac{2}{3} n_f; \quad c_0 = \frac{1}{2}; \\ b_1 &= \frac{1}{2} \frac{51N_c - 19n_f}{11N_c - 2n_f}; \quad c_1 = \frac{1}{72} (101N_c - 10n_f) \end{aligned} \quad (3.6)$$

In our calculation we adopt  $\overline{m}_b(r)_{1\text{ loop}}$  in Eq.(3.4) and  $\overline{m}_b(r)_{2\text{ loop}}$  in Eq.(3.5) as the  $\overline{m}_b(r)$  mass for the LO and NLO cross sections, respectively [31]. The renormalization of the bottom quark mass in Yukawa coupling is defined as

$$m_b^0 = \overline{m}_b(r) \left( 1 + \frac{\text{SM like}}{\text{SUSY}} \right); \quad (3.7)$$

where the counterterm of the SM-like QCD part  $\frac{\text{SM like}}{\text{SUSY}}$  is calculated in  $\overline{MS}$  scheme, while SUSY counterterm part  $\frac{\text{SUSY}}{\text{SUSY}}$  is calculated in on-shell(OS) scheme. Due to the fact that there are significant corrections to bH coupling for large value of  $\tan\beta$ , we absorb these corrections in the Yukawa coupling [32]. The resummed bH Yukawa coupling can be expressed as [17, 30, 33]

$$g_{bH} = p \frac{igV_{cb}}{2m_W} m_c \cot P_R + \overline{m}_b(r) \frac{1}{1 - \frac{\tan\beta}{b}} \tan P_L; \quad (3.8)$$

where

$$\begin{aligned}
 b &= \frac{m_b}{1 + \frac{1}{1}}; \\
 m_b &= \frac{2}{3} \frac{s}{m_{\tilde{g}}} \tan I(m_{\tilde{b}_3}^2; m_{\tilde{b}_2}^2; m_{\tilde{g}}^2); \\
 1 &= \frac{2}{3} \frac{s}{m_{\tilde{g}}} A_b I(m_{\tilde{b}_1}^2; m_{\tilde{b}_2}^2; m_{\tilde{g}}^2); \\
 I(a; b; c) &= \frac{ab \log \frac{a}{b} + bc \log bc + ca \log \frac{c}{a}}{(a-b)(b-c)(c-a)}; \tag{3.9}
 \end{aligned}$$

Since in the calculation of the cross section of the process  $pp \rightarrow b\bar{b}H \rightarrow X$  at the tree-level, we used the resummed  $b\bar{b}H$  Yukawa coupling, we have to add a finite renormalization of the bottom quark mass in  $b\bar{b}H$  Yukawa coupling to avoid double counting in the SUSY QCD NLO corrections to the cross section [34].

$$m_b \rightarrow \overline{m}_b(r) [1 + \frac{H_b}{b}] + O(\frac{2}{s}); \tag{3.10}$$

$$\frac{H_b}{b} = \frac{2}{3} \frac{s}{m_{\tilde{g}}} (1 + \frac{1}{\tan^2}) m_{\tilde{g}} \tan I(m_{\tilde{b}_1}^2; m_{\tilde{b}_2}^2; m_{\tilde{g}}^2); \tag{3.11}$$

For the renormalization of the strong coupling constant  $g_s$ , we divide the counterterm of the strong coupling constant into two terms: SM-like QCD term and SUSY term ( $g_s = g_s^{(SM \text{ like})} + g_s^{(SUSY)}$ ), and the explicit expressions of these two terms can be obtained by adopting  $\overline{MS}$  scheme at renormalization scale  $r$  [17, 28].

$$\frac{g_s^{(SM \text{ like})}}{g_s} = \frac{s(r)}{4} \frac{\frac{(SM \text{ like})}{0}}{2} \frac{1}{1} + \frac{1}{3} \ln \frac{m_t^2}{r^2} \frac{\#}{\#}; \tag{3.12}$$

$$\frac{g_s^{(SUSY)}}{g_s} = \frac{s(r)}{4} \frac{\frac{(SUSY)}{0}}{2} \frac{1}{1} + \frac{N_c}{3} \ln \frac{m_{\tilde{g}}^2}{r^2} + \frac{\mathbb{X}^{1/2}}{U=u;c;t} \frac{1}{12} \ln \frac{m_U^2}{r^2} + \frac{\mathbb{X}^{1/2}}{D=d;s;b} \frac{1}{12} \ln \frac{m_D^2}{r^2} \frac{\#}{\#}; \tag{3.13}$$

where we have used the notations

$$0^{(SM \text{ like})} = \frac{11}{3} N_c - \frac{2}{3} n_f - \frac{2}{3}; \quad 0^{(SUSY)} = \frac{2}{3} N_c - \frac{1}{3} (n_f + 1); \tag{3.14}$$

The number of colors  $N_c$  equals 3, the number of active flavors is taken to be  $n_f = 5$  and  $1 = 1_{UV} - E + \ln(4)$ . The summation is taken over the indexes of squarks and generations. Since the  $\overline{MS}$  scheme violates supersymmetry, it is necessary that the  $q\bar{q}$  Yukawa coupling  $g_s$ , which should be the same with the  $q\bar{q}$  gauge coupling  $g_s$  in the supersymmetry, takes a finite shift at one-loop order as shown in Eq.(3.15) [29].

$$g_s = g_s \left( 1 + \frac{s}{8} - \frac{4}{3}N_c C_F \right); \quad (3.15)$$

with  $C_F = 4/3$ . In our numerical calculation we take this shift between  $g_s$  and  $g_s$  into account.

The SUSY QCD one-loop Feynman diagrams for both  $q\bar{q} \rightarrow b\bar{b}H$  and  $gg \rightarrow b\bar{b}H$  subprocesses can be divided into virtual gluon/quark exchange part (SM-like) and virtual gluino/squark exchange part (SUSY). We express the renormalized amplitudes for both subprocesses as

$$M_{\text{virtual}}^{q\bar{q}gg} = M_{\text{SM-like}}^{q\bar{q}gg} + M_{\text{SUSY}}^{q\bar{q}gg} \quad (3.16)$$

Then the SUSY QCD NLO contributions to the cross sections of the subprocesses  $q\bar{q} \rightarrow gg + b\bar{b}H$  can be expressed as

$$\hat{M}_{\text{virtual}}^{q\bar{q}gg} = \frac{Z}{d_3} \overline{M}_{\text{tree}}^{q\bar{q}gg} (2Re(M_{\text{tree}}^{q\bar{q}gg} M_{\text{virtual}}^{q\bar{q}gg}) + \overline{|M_{\text{tree}}^{q\bar{q}gg}|^2}); \quad (3.17)$$

where  $d_3$  is three-body phase space element,  $M_{\text{tree}}^{q\bar{q}}$  and  $M_{\text{tree}}^{gg}$  are the Born amplitudes for  $q\bar{q} \rightarrow gg + b\bar{b}H$  subprocesses separately, and  $M_{\text{virtual}}^{q\bar{q}}$  and  $M_{\text{virtual}}^{gg}$  are their renormalized amplitudes of the SUSY QCD one-loop diagrams. The bar over the summation in Eq.(3.17) recalls averaging over initial spin and color states.

$\hat{\sigma}_{\text{virtual}}^{\text{qqgg}}$  are free of UV divergences but contain soft/collinear IR divergences, among them the soft IR divergence can be cancelled by adding with the soft real gluon emission corrections. The soft and collinear singularities from real gluon emission subprocess can be conveniently isolated by slicing the phase space into different regions defined with suitable cuts[35]. We introduce an arbitrary soft cut  $s (2E_g = \frac{p}{\hat{s}})$  with small value to separate the phase space of the gluon emission 2 ! 4 subprocess into two regions, i.e., soft and hard gluon emission regions. Then for the gluon emission 2 ! 4 subprocesses based on  $(q\bar{q}; q^0\bar{q}^0; gg) \rightarrow b\bar{c}H$ , ( $q = u; d; q^0 = s; c$ ), we have

$$\begin{aligned} \hat{\sigma}_{\text{real}}((q\bar{q}; q^0\bar{q}^0; gg) \rightarrow b\bar{c}H \rightarrow g) &= \hat{\sigma}_{\text{soft}}((q\bar{q}; q^0\bar{q}^0; gg) \rightarrow b\bar{c}H \rightarrow g) \\ &+ \hat{\sigma}_{\text{hard}}((q\bar{q}; q^0\bar{q}^0; gg) \rightarrow b\bar{c}H \rightarrow g); \end{aligned} \quad (3.18)$$

where  $\hat{\sigma}_{\text{soft}}$  is obtained by integrating over the soft region of the emitted gluon phase space, and contains all the soft IR singularities. Furthermore, we decompose each cross section of  $\hat{\sigma}_{\text{hard}}$  for hard-gluon emission subprocesses  $q\bar{q} \rightarrow q^0\bar{q}^0 \rightarrow gg \rightarrow b\bar{c}H \rightarrow g$  and light-quark emission subprocesses  $\hat{\sigma}_{\text{real}}$  for  $(q\bar{q}; gg) \rightarrow b\bar{c}H \rightarrow (q; q)$ , into a sum of collinear and non-collinear terms to isolate the remaining collinear singularities from  $\hat{\sigma}_{\text{hard}}$  and  $\hat{\sigma}_{\text{real}}$ , by introducing another cut  $c$  called collinear cut.

The cross sections in the non-collinear hard-gluon/light-quark emission regions, can be obtained by performing the phase space integration in 4-dimension by using Monte Carlo method. Then we get the SUSY QCD NLO corrected cross sections for subprocesses  $q\bar{q} \rightarrow q^0\bar{q}^0 \rightarrow gg \rightarrow b\bar{c}H$  as follows. For  $q\bar{q}$  annihilation ( $q = u; d$ ) sub-

processes,

$$\begin{aligned}\hat{\sigma}_{\text{loop}}(\text{qq} \rightarrow \text{bH} + \text{X}) &= \hat{\sigma}_{\text{tree}}(\text{qq} \rightarrow \text{bH} + \text{X}) + \hat{\sigma}_{\text{virtual}}(\text{qq} \rightarrow \text{bH} + \text{X}) \\ &+ \sum_{\substack{\text{ij} = \text{qq}; \\ \text{ij} = \text{qg}; \\ \text{ij} = \text{gg}}} \hat{\sigma}_{\text{real}}(\text{ij} \rightarrow \text{bH} + \text{g}; \text{q}; \text{q});\end{aligned}\quad (3.19)$$

while for  $q^0\bar{q}^0$  annihilation ( $q^0 = c; s$ ) and gg fusion subprocesses,

$$\begin{aligned}\hat{\sigma}_{\text{loop}}(q^0\bar{q}^0 \rightarrow \text{gg} + \text{bH} + \text{X}) &= \hat{\sigma}_{\text{tree}}(q^0\bar{q}^0 \rightarrow \text{gg} + \text{bH} + \text{X}) + \hat{\sigma}_{\text{virtual}}(q^0\bar{q}^0 \rightarrow \text{gg} + \text{bH} + \text{X}) \\ &+ \hat{\sigma}_{\text{real}}(q^0\bar{q}^0 \rightarrow \text{gg} + \text{bH} + \text{g});\end{aligned}\quad (3.20)$$

The remaining collinear IR divergences in Eq.(3.19) and Eq.(3.20) are absorbed into the parton distribution functions, separately. Then the SUSY QCD NLO corrected total cross section for  $\text{pp} \rightarrow \text{bH} + \text{X}$  process  $_{\text{loop}}$ , can be obtained by using Eq.(3.1) and replacing  $\hat{\sigma}_{\text{tree}}^{\text{ij}}(\text{ij} \rightarrow \text{bH} + \text{X})$ , ( $\text{ij} = \text{qq}; q^0\bar{q}^0; \text{gg}$ ) by  $\hat{\sigma}_{\text{loop}}(\text{ij} \rightarrow \text{bH} + \text{X})$ , ( $\text{ij} = \text{qq}; q^0\bar{q}^0; \text{gg}; \text{qg}; \text{gg}$ ), and CTEQ 6L1 parton distribution functions by CTEQ 6M ones[26]. The total cross section  $_{\text{loop}}(\text{pp} \rightarrow \text{bH} + \text{X})$  up to SUSY QCD NLO should be independent on the two arbitrary cuts  $s_s$  and  $c_c$ . In our both analytical and numerical calculations, we checked the cancellations of the UV and IR divergences, and found that the final results are both UV- and IR-finite.

## IV Numerical Results and Discussions

In this section, we present some numerical results of the total and differential cross sections of the process  $\text{pp} \rightarrow \text{bH} + \text{X}$  inspired by the squark-mixing loop contributions at the LHC. We take the SM parameters as:  $m_W = 80.425 \text{ GeV}$ ,  $m_Z = 91.1876 \text{ GeV}$ ,  $m_t = 175 \text{ GeV}$ ,  $m_b = 4.7 \text{ GeV}$ ,  $m_c = 1.2 \text{ GeV}$ ,  $m_s = 0.15 \text{ GeV}$ ,

$V_{cb} = 0.04$ ,  $V_{ub} = 0.0035$ ,  $V_{cd} = 0.222$ ,  $V_{cs} = 0.97415$ ,  $V_{cb} = 0.04$  and  $V_{tb} = 0.99915$  [36] and neglect the light-quark masses ( $m_{u,d}$ ) in the numerical calculation. The value of the fine structure constant at the energy scale of  $Z^0$  pole mass, is taken as  $\alpha_w(m_Z) = 127.918$  [36]. We use the CTEQ 6L1 and CTEQ 6M parton distribution functions for the calculations of LO and NLO contributed cross sections, respectively [26]. The colliding energy of proton-proton collider at the LHC is  $\frac{p}{s} = 14 \text{ TeV}$ . We fix the value of the renormalization/factorization scale being  $Q = Q_0 = r = f$  for simplicity, where  $Q_0$  is defined to be a half of the final particle masses. As a numerical demonstration, we refer to the relevant MSSM parameters of Snowmass point SPS 4 with high  $\tan \beta$  [37, 38] except considering the left-handed up-type squark mixings in the MSSM. SPS 4 is a mSUGRA point with input parameters:

$$m_0 = 400 \text{ GeV}; m_{1=2} = 300 \text{ GeV}; A_0 = 0; \tan \beta = 50; \mu > 0; \quad (4.1)$$

Since the squark sector in Snowmass points doesn't include squark mixing, we don't adopt the SPS 4 physical sparticle spectrum, but the ISA JET [39] equivalent input MSSM parameters at this benchmark point, with which one can reproduce the ISA JET spectrum with SUSYGEN [40] and PYTHIA [41]. These relevant MSSM parameters at SPS 4 point we used in our calculation, are listed below [38].

$$\begin{aligned} \tan \beta &= 50; m_H^0 = 416.28 \text{ GeV}; m_g = 721.03 \text{ GeV}; \\ m_{u_L} &= m_{d_L} = m_{e_L} = m_{s_L} = 732.2 \text{ GeV}; m_{b_L} = m_{t_L} = 640.09 \text{ GeV}; \\ m_{u_R} &= m_{e_R} = 716.00 \text{ GeV}; m_{d_R} = m_{s_R} = 713.87 \text{ GeV}; m_{b_R} = 673.40 \text{ GeV}; \\ m_{\tilde{t}_R} &= 556.76 \text{ GeV}; A_t = 552.20 \text{ GeV}; A_b = 729.52 \text{ GeV}; \end{aligned} \quad (4.2)$$

The squark-mixing parameters  $\alpha_{12}$ ,  $\alpha_{31}$  and  $\alpha_{23}$  are constrained by low energy data on FCNC [21]. Following the reference [21], we use the bounds for the squark-mixing parameters as

$$\begin{aligned}\alpha_{12} &< 0.1^p \frac{m_{\tilde{u}} m_{\tilde{c}}}{m_{\tilde{u}} m_{\tilde{c}}} = 500 \text{ GeV}; \\ \alpha_{31} &< 0.098^p \frac{m_{\tilde{u}} m_{\tilde{c}}}{m_{\tilde{u}} m_{\tilde{c}}} = 500 \text{ GeV}; \\ \alpha_{23} &< 8.2 \frac{m_{\tilde{c}} m_{\tilde{t}}}{(500 \text{ GeV})^2};\end{aligned}\quad (4.3)$$

Considering above limitations on squark-mixing parameters, in our calculations we use the MSSM parameters shown in Eq.(4.2) and take  $\alpha_{12} = 0.03$ ,  $\alpha_{31} = 0.03$  and  $\alpha_{23} = 0.6$ , which satisfy the constraints of Eq.(4.3), if there is no di erent statement. Actually, our calculation shows that the cross section involving NLO QCD corrections for process  $pp \rightarrow b\bar{b}H \rightarrow X$  is mostly related to the squark-mixing parameter  $\alpha_{23}$ , but not sensitive to the  $\alpha_{12}$  and  $\alpha_{31}$ . That implies the contributions from the  $\alpha_L$ - $\alpha_L$  and  $\alpha_L$ - $\alpha_L$  squark-mixings are very small in our chosen parameter space.

In numerical calculation, we put the cuts on the transverse momenta of final bottom, charm quarks and charged Higgs boson as

$$|\vec{p}_T^b| > 20 \text{ GeV}; \quad |\vec{p}_T^c| > 20 \text{ GeV}; \quad |\vec{p}_T^H| > 10 \text{ GeV}; \quad (4.4)$$

As we discussed in above section, the final results should be independent on cutos  $s_s$  and  $c_c$ . That is also one of the checks of the correctness of our calculation. We checked the independence of cutos  $s_s$  and  $c_c$  in our calculation. In the following numerical calculation we  $x_s = 10^{-3}$  and  $x_c = 10^{-5}$ .

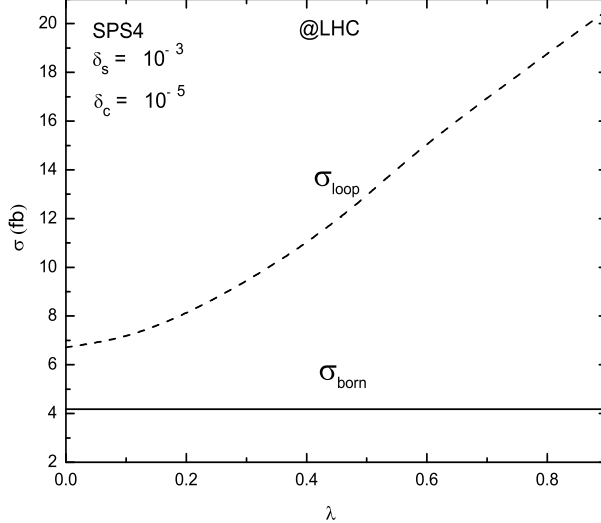


Figure 3: The cross sections for the process  $pp \rightarrow bH + X$  at the tree-level( $\sigma_{tree}$ ) and up to QCD one-loop level( $\sigma_{loop}$ ) as the functions of the mixing strength parameter ( $\lambda$ ) in the up-type squark mass matrix at the LHC. The relevant MSSM parameters at the Snowmass point SPS 4 are adopted (shown in Eq.(4.2)).

In Fig.3 we present the total cross sections for the process  $pp \rightarrow bH + X$  at the tree-level( $\sigma_{tree}$ ) and up to SUSY QCD NLO ( $\sigma_{loop}$ ) as the functions of the mixing strength between  $g_L$  and  $\tilde{t}_L$ , ( $\lambda$ ), at the LHC with the relevant MSSM parameters at the Snowmass point SPS 4 shown in Eq.(4.2). We can see the one-loop correction significantly enhances the corresponding LO cross section (solid curve), and loop contribution goes up with the increment of the mixing parameter  $\lambda$ . As we know the tree-level cross section for  $pp \rightarrow bH + X$  process is suppressed by CKM matrix element in the Yukawa coupling of  $bH$ . But the mixing between  $g_L$  and  $\tilde{t}_L$  in the SUSY soft-breaking sector can make the one-loop contributions quite sizable, and significantly increases the tree-level cross section by a factor of 1.5 – 5, which is shown in Fig.3.

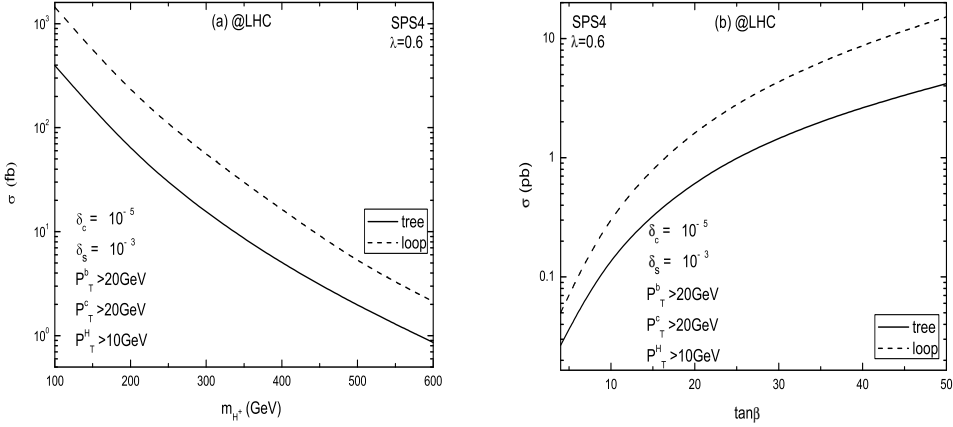


Figure 4: The cross sections for the process  $pp \rightarrow b d H + X$  at the tree-level  $_{tree}$  and up to SUSY QCD NLO  $_{loop}$  as the functions of the mass of charged Higgs boson (Fig.4 (a)) and the ratio of the vacuum expectation values  $\tan\beta$  (Fig.4 (b)). The other relevant MSSM parameters are taken from the Snowmass point SPS 4 listed in Eq.(4.2).

In Fig.4 we depict the cross sections for the process  $pp \rightarrow b d H + X$  at the tree-level and up to SUSY QCD NLO at the LHC as the functions of the mass of charged Higgs boson in Fig.4 (a) and the ratio of the vacuum expectation values  $\tan\beta$  in Fig.4 (b) respectively, by taking the other MSSM parameter values from the Snowmass point SPS 4 (see Eq.(4.2)). We can read from Fig.4 (a) that when  $m_H$  increases from 100 GeV to 600 GeV, the total NLO QCD cross section decreases from 1.548 pb to 0.86 fb at the LHC, while the tree-level cross section decreases from 0.40 pb to 0.86 fb. We can see that if the MSSM scenario with left-handed up-type squark mixings is really true, the LHC machine with an integrated luminosity of about  $100 \text{ fb}^{-1}$  can have the potential to find the signature of charged Higgs boson via the process  $pp \rightarrow b d H + X$  with  $m_H$  in the range of [100 GeV; 600 GeV].

Fig.4 (b) shows that with  $m_H = 416.28$  GeV the cross section up to the  $O(gg_s^4)$  order loop increases from 0.05 fb to 15.18 fb, as  $\tan\theta$  varies from 4 to 50, while the tree-level cross section is much smaller than loop. We can conclude that the production rate of the single charged Higgs bosons associated with bottom-charm quark pair at the LHC, can be enhanced by the gluino/squark loop contributions in the MSSM with squark-mixing structure.

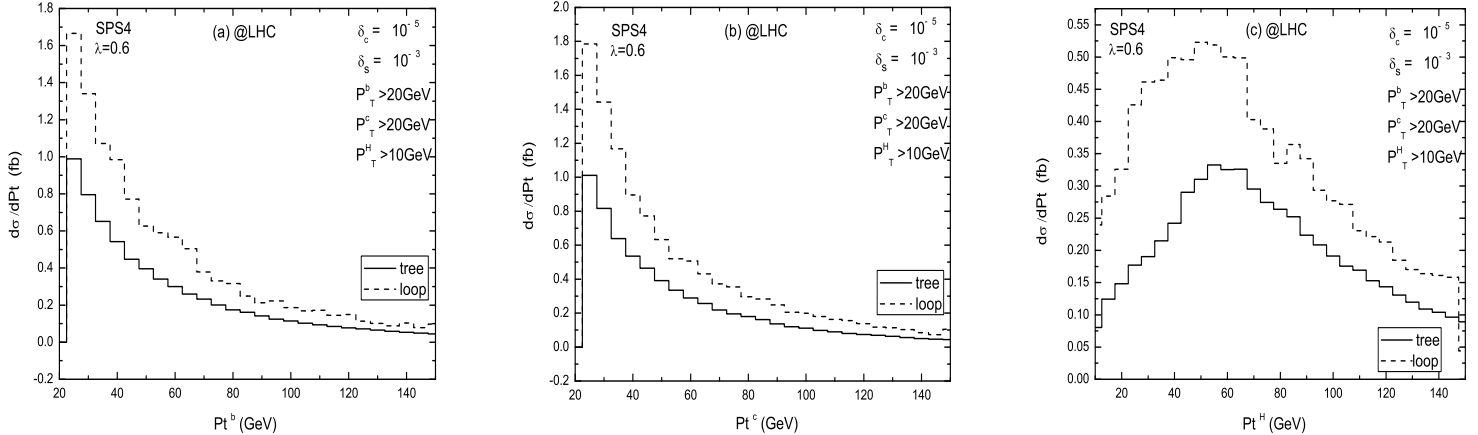


Figure 5: The differential cross sections of the  $pp \rightarrow b\bar{b}H + X$  process at the tree-level( $O(gg_s^2)$ ) and up to the SUSY QCD NLO ( $O(gg_s^4)$ ) as the functions of (a) the transverse momentum of bottom-quark  $p_T^b$ , (b) the transverse momentum of charm-quark  $p_T^c$ , and (c) the transverse momentum of the charged Higgs boson  $p_T^H$  at the LHC, with the relevant parameters of the Snowmass point SPS 4 (shown in Eq.(4.2)).

In Figs.5 (a-c) we present the distributions of the differential cross sections  $d\sigma_{tree,loop} = dp_T^b$ ,  $d\sigma_{tree,loop} = dp_T^c$ ,  $d\sigma_{tree,loop} = dp_T^H$  for the process  $pp \rightarrow b\bar{b}H + X$  in the MSSM with left-handed up-type squark-mixing structure and the relevant parameters at the Snowmass point SPS 4 (shown in Eq.(4.2)) at the LHC. These figures demonstrate that the loop contributions up to the order ( $O(gg_s^4)$ ) can significantly enhance the

tree-level differential cross sections  $d_{tree} = dp_T^b$ ,  $d_{tree} = dp_T^c$  and  $d_{tree} = dp_T^H$  at the LHC. We find that in the low  $p_T^b$  and  $p_T^c$  regions the corresponding differential cross section values including SUSY QCD NLO corrections can be very large.

## V Summary

The general three-family up-type squark mass matrix originating from the soft SUSY breaking sector, can induce the cross section enhancement for the  $pp \rightarrow b\bar{b}H^+ + X$  process at one-loop level. In this paper we investigate the flavor changing effects on the production of single charged Higgs bosons in association with b-c quark pair in the framework of the MSSM with left-handed up-type squark mixings. We analyze the dependence of the cross section involving NLO QCD corrections for  $pp \rightarrow b\bar{b}H^+ + X$  process on the charged Higgs boson mass  $m_H$ , the ratio of the vacuum expectation values  $\tan\beta$ , and the distributions of the transverse momenta of bottom-quark  $p_T^b$ , charm-quark  $p_T^c$  and charged Higgs boson  $p_T^H$  at the CERN LHC. We find that the one-loop contributions are mostly inspired by the mixing of the  $c_L$ - $t_L$  sector, and the QCD NLO corrections can significantly enhance the corresponding tree-level( $O(gg_s^2)$ ) cross sections in the MSSM with squark-mixings. Our numerical results show the corrected cross section can reach the value of 1.548 pb in our chosen parameter space. With this production rate we may discriminate models of flavor symmetry breaking and reveal new exciting discovery channel for the signature of single charged Higgs boson at the LHC.

**Acknowledgments:** This work was supported in part by the National Natural

Science Foundation of China, the Education Ministry of China and a special fund sponsored by Chinese Academy of Sciences.

## References

- [1] S.L. Glashow, Nucl. Phys. 22, (1961)579; S. Weinberg, Phys. Rev. Lett. 1, (1967)1264; A. Salam, Proc. 8th Nobel Symposium Stockholm 1968, ed. N. Svartholm (Almqvist and Wiksell, Stockholm 1968) p.367; H.D. Politzer, Phys. Rep. 14 (1974)129.
- [2] S.L. Glashow and S. Weinberg, Phys. Rev. D 15, (1977)1958.
- [3] H.E. Haber and G.L. Kane, Phys. Rep. 117, (1985)75; J.F. Gunion and H.E. Haber, Nucl. Phys. B 272, (1986)1.
- [4] J.F. Gunion, H.E. Haber, G.L. Kane and S. Dawson, "The Higgs Hunter's Guide", SCIPP-89/13, Addison-Wesley, Menlo Park, 1990.
- [5] F. Gabbiani and A. Masiero, Nucl. Phys. B 322 (1989)235; F. Gabbiani, E. Gabrielli, A. Masiero and L. Silvestrini, Nucl. Phys. B 477 (1996)321, hep-ph/9604387; M. Misiak, S. Pokorski and J. Rosiek, Adv. Ser. Direct. High Energy Phys. 15 (1998)795, hep-ph/9703442.
- [6] B. Abbott et al. [D0 Collaboration], Phys. Rev. Lett. 82 (1999)4975; F. Abe et al. [CDF Collaboration], Phys. Rev. Lett. 79 (1999)357.

[7] A A . Barrientos Bendezu and B A . Kniehl, Nucl. Phys. B 568 (2000)305; O . Brein and W . Hollik, Eur. Phys. J. C 13 (2000)175; JF . Gunion, H E . Haber, F E . Paige, W K . Tung and S S . W illenbrock, Nucl. Phys. B 294 (1987)621; S S D . W illenbrock, Phys. Rev. D 35 (1987)173; A . Krause, T . P lehn, M . Spira and P M . Zerwas, Nucl. Phys. B 519 (1998)85.

[8] Y . Jiang, W .-G . Ma, L . Han and Z .-H . Yu, J. Phys. G 23 (1997) 385, Erratum , ibidem G 23 (1997)1151; A . Belyaev, M . D rees, O . J P . Eboli, J K . M izukoshi and S F . N ovaes, Phys. Rev. D 60 (1999)075008; A . Belyaev, M . D rees and J K . M izukoshi, Eur. Phys. J. C 17 (2000)337; H .-S . Hou, W .-G . Ma, R .-Y . Zhang, Y . Jiang, L . Han, and L .-R . X ing, Phys. Rev. D 71 (2005)075014; S . M oretti, J. Phys. G 28 (2002)2567.

[9] E . Eichten, I . Hindli e, K D . Lane and C . Quigg, Rev. Mod. Phys. 56 (1984)579 [Addendum ibid. 58 (1986) 1065]; N . G . D eshpande, X . Tata and D . A . D icus, Phys. Rev. D 29 (1984) 1527; W .-G . Ma, C .-S . Li, and L . Han, Phys. Rev. D 53 (1996)1304; S .-H . Zhu, C .-S . Li, and C .-S . G ao, Phys. Rev. D 58 (1998)055007.

[10] D A . D icus, J L . Hewett, C . Kao and T G . Rizzo, Phys. Rev. D 40 (1989)787; A A . Barrientos Bendezu and B A . Kniehl, Phys. Rev. D 59 (1998)015009, and Phys. Rev. D 63 (2001) 015009; O . Brein, W . Hollik and S . Kanemura, Phys. Rev. D 63 (2001)095001; W . Hollik and S .-H . Zhu, Phys. Rev. D 65 (2002)075015.

[11] J. Gunion, G. Ladinsky, C.-P. Yuan, et al, Snowmass Summer Study 1990:0059-81 (QCD 161:15:1990); V. Barger, R.J.N. Phillips and D.P. Roy, Phys. Lett. B 324 (1994)236; F. Borzumati, J. Kneur, N. Polonsky, Phys. Rev D 60 (1999)115011; A. Belyaev, D. Garcia, J. Guasch, J. Sola, Phys. Lett. B 530 (2002)179, hep-ph/0103178.

[12] J.L.Diaz-Cruz, H.-J. He, C.-P. Yuan, Phys. Lett. B 530 (2002)179, hep-ph/0103178.

[13] K.A. Assamagan, Y. Coadou and A. Deandrea, Eur. Phys. J.C 4 (2002)1; P. Salmi, R. Kinnunen, and N. Stepanov, CMS Note 2002/024, hep-ph/0301166; K.A. Assamagan and N. Gollub, Eur. Phys. J. C 39S2 (2005)25, hep-ph/0406013.

[14] K.A. Assamagan and Y. Coadou, Acta Phys. Polon B 33 (2002)707; R. Kinnunen and A.N. Kitenko, Report CMS Note 2003/006.

[15] S.H. Zhu, Phys. Rev D 67 (2003) 075006.

[16] E.L. Berger, T. Han, J. Jiang, T. Plehn, Phys. Rev D 71 (2005)115012.

[17] P. Wu, W.-G. Ma, R.-Y. Zhang, Y. Jiang, L. Han, L. Guo, Phys. Rev. D 73 (2006)015012, hep-ph/0601069.

[18] H.-J. He and C.-P. Yuan, Phys. Rev. Lett. 83 (1999)28, hep-ph/0203090.

[19] W. Hollk, S. Penaranda, M. Vogt, Eur. Phys. J. C 47 (2006)207-217.

[20] See, e.g., Z. X. iong and J. M. Yang, Nucl. Phys. B 628 (2002) 193; C. Bobeth, T. Ewerth, F. K. riger, J. U. rban, Phys. Rev. D 66 (2002) 074021, hep-ph/0204225; S. Rai Choudhury, Naveen Gaur and Namit Mahajan, Phys. Rev. D 66 (2002) 094015, Phys. Rev. D 66 (2002) 054003, hep-ph/0203041; S. Rai Choudhury and Naveen Gaur, hep-ph/0206128; hep-ph/0205076; hep-ph/0207353.

[21] See, e.g., F. Gabbiani, E. Gabrielli, A. Masiero, L. Silverstrini, Nucl. Phys. B 477 (1996) 321; M. Misiak, S. Pokorski, J. Rosiek, Adv. Ser. Direct. High Energy Phys. 15, 795 (1998); F. Borzumati, C. Greub and T. Hurth, Phys. Rev. D 62 (2000) 075005; T. Beuster, C. Greub and T. Hurth, Nucl. Phys. B 609 (2001) 359.

[22] M. J. Duncan, Nucl. Phys. B 221 (1983) 285; Phys. Rev. D 31 (1985) 1139.

[23] K. Hikasa and M. Kobayashi, Phys. Rev. D 36 (1987) 724.

[24] T. P. Cheng and M. Sher, Phys. Rev. D 35, 3484 (1987).

[25] See, e.g., S. D. mopoulos, D. Sutter, Nucl. Phys. B 452 (1996) 496; F. Gabbiani, et al., Nucl. Phys. B 477 (1996) 421; M. Misiak, S. Pokorski, J. Rosiek, Adv. Ser. Direct. High Energy Phys. 15 (1998) 795.

[26] H. L. Lai et al. (CTEQ), Eur. Phys. J. C 12 (2000) 375.

[27] A. Denner, Fortschr. Phys. 41 (1993) 4, 307.

[28] L. Reina, S. Dawson, D. Wackerlo, Phys. Rev. D 65 (2002) 053017.

[29] W . Beenakker, R . Hopker, P M . Zerwas, Phys.Lett.B 378 (1996)159; W . Beenakker, R . Hopker, T . P lehn, P M . Zerwas, Z Phys.C 75 (1997)349.

[30] M . Carena, D . Garcia, U . N ierste and C E . W agner, Nucl. Phys. B 577 (2000)88.

[31] S . Dawson, C B . Jackson, L . Reina and D . W ackerlo, Phys. Rev. D 69 (2004)074027.

[32] L J.H all, R .R attazzi and U .S arid, Phys. Rev.D 50 (1994)7048; R .H emp ing, Phys. Rev.D 49 (1994)6168; M .C arena, M .O lechowski, S .P okorski and C E M . W agner, Nucl. Phys. B 426 (1994)269; D .P ierœ, J. Bagger, K .M atchev and R .Zhang, Nucl. Phys. B 491 (1997)3.

[33] J .G uasch, P .H a iger, M .S pira, Phys. Rev.D 68 (2003)115001.

[34] P .H a iger and M .S pira, Nucl. Phys.B 719 (2005)35.

[35] W .T .G iele and E W .N .G lover, Phys. Rev.D 46 (1992)1980; W .T .G iele, E W .G lover and D A .K osower, Nucl. Phys.B 403 (1993)633; S .K eller and E .L aenen, Phys. Rev.D 59114004 (1999).

[36] S .E idem an, et al, Phys. Lett. B 592 (2004)1.

[37] B .C .A llanach et al, Eur.Phys.J.C 25 (2002)113; eConfC 010630 (2001) P 125.

[38] N abil G hodbane, H ans-U lrich M artyn, hep-ph/0201233.

[39] H .B aer et al, hep-ph/0001086, JSA JET , <http://paige.home.cern.ch/paige>

[40] N .G hodbane et al, LY CEN 9992, hep-ph/9909499, SUSYGEN ,<http://lyoinfo.in2p3.fr/susygen/susygen>

[41] T .S jstrand et al, LU TP 01-21, hep-ph/0108264, PYTHIA ,<http://www.thep.lu.se/~torbjorn/Pythia>